32nd URSI GASS, Montreal, 19-26 August 2017

Meteoroid Sputtering, High-Altitude Radar and Optical Meteors, and Sources for Lower-Thermospheric Metals

J.D. Mathews*(1), B. Gao(1), V. Kesaraju(1), S. Raizada(2)
(1) Radar Space Sciences Lab, 323A EE East, The Pennsylvania State Un., University Park PA 16802-2707 USA, JDMathews@psu.edu
(2) Space Science Division, Arecibo Observatory/SRI, Puerto Rico USA

Abstract

Observations of radar and optical meteors at altitudes above the ablation-defined meteor zone point to a "new" sputtering source of high-altitude metals while also yielding clues to the radio science of radar meteors. That high-altitude radar meteors (HARMs) are visible at altitudes of up ~180 km using the 50 MHz Jicamarca Radio Observatory (JRO) implies that a significant fraction of the directly-sputtered meteoroid material is ionized as the collisional mean free path (MFP) at these altitudes is many tens of meters. Also, that high-altitude **k**⊥**B** FAI (Field-Aligned Irregularity) trail-echoes are observed in association with HARM head-echoes offers insight into the meteor-associated plasma processes as well as the radar scattering mechanism. In particular, HARMs reveal the onset, as the meteoroid enters the upper atmosphere, of radar scattering which must be from the minimum, radar detectible, electron production. The maximum Radar backscattering Cross-Section (RCS) from N electrons, $\sigma_{BS} = 4\pi r_e^2 N^2$, is the result of totally coherent scattering from N, equally illuminated and closely spaced, electrons where r_e is the classical electron radius. An estimate for N is given. Overall, this approach yields a direct, physics-based path linking the RCS of observed head- and trail-echoes to the meteoroid sputtering process and to the ion atmospheric "capture" process whereby the head-echo "plasma" is embedded into the atmosphere.

In addition, recent lidar observations of atomic Fe, Na, and K at altitudes well above the traditional meteor zone violate the usual assumptions regarding thermospheric metals and form an instructive complication to the above "simple meteoroid" scenario as many meteoroids appear to be fragmenting at high altitudes. This "cold fragmentation" likely points to complex "dirty-ice" and "dust-ball" meteoroids comprised of small, dense grains weakly bound together by more volatile substances. These meteoroids may disperse into an extended "coma" that presents a more complex and larger surface area atmospheric-interaction region. We briefly discuss sputtering, the impact energies needed for onset of sputtering, sputtering yield, and the observational evidence available for interpretation of meteoroid sputtering as a source of aeronomically interesting metals above the classical meteor zone. We further suggest that a thermospheric "reservoir" of nanometer-sized dust play an important aeronomic role.

1. Introduction

High Altitude Optical Meteors (HAOMs) have been discussed in the literature for some time [1]. An example event frame from a Low-Light TV telescopic observing system is shown in Fig. 1.

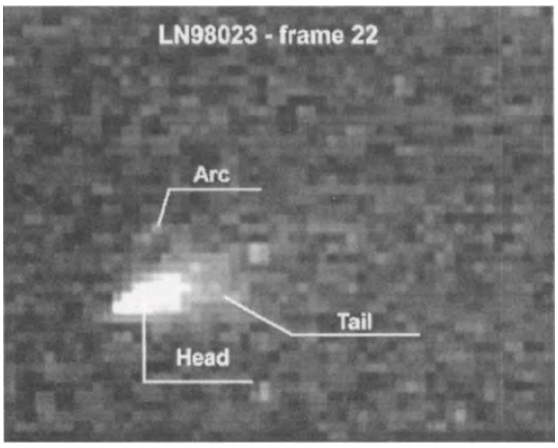

Figure 1. A High-Altitude Optical Meteor (HAOM) at 150.4 km altitude [1, Figure 2]. This event shows remarkable structure (indicated) made visible through sputtering interaction [2] of the meteoroid with the atmosphere.

High-Altitude Radar Meteors (HARMs) have been observed at the Jicamarca Radio Observatory (JRO) [3,4] with an example shown in Figure 2. Shown here is a spectacular high-altitude, head-echo (HARM) event that passes through the **k**⊥**B** region near 135 km and spans ~60 km in range. Almost the entire atmospheric (nearly "down-the-beam") trajectory of this meteoroid that has a radial speed of ~60.33 km/s is seen. The transition from sputtering to ablation occurs below ~120 km. Both the initial head-echo plasma (traveling with the meteoroid) and the trail-echo plasma are generated well above the ablation zone and signal the creation and deposition of electrons (& ions) and, almost certainly, nanometer dust particles. The relatively long-lived high-altitude trail echoes in the **k**⊥**B** region are often observed without the progenitor head-echo [3]. Approximately 90 HARM

events were observed over ~7 hours of two separate pre-dawn observing periods.

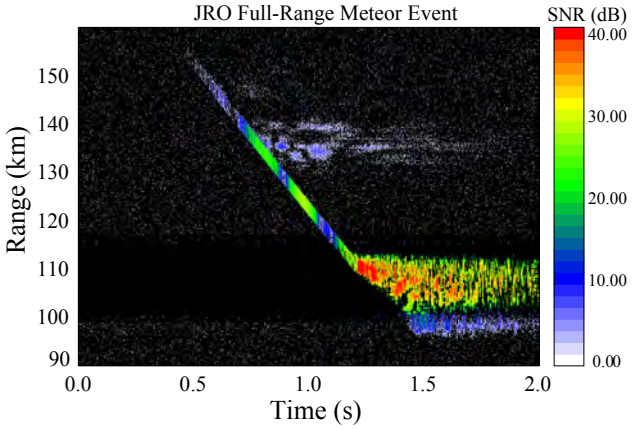

Figure 2. A High-Altitude Radar Meteor (HARM) event observed using the JRO 50 MHz radar system [3,4]. This event begins well above the ablative meteor zone and ends with a terminal flare just below 100 km altitude. In this figure the Equatorial Electrojet (EEJ) region FAI (Field-Aligned Irregularity) returns have been removed [4] clearly revealing the Range-Spread Trail Echo (RSTE) in the 100-112 km region. The trail-scattering region between 130-140 km reveals the extent of sputtered ionization embedded in the atmosphere at the radar $\mathbf{k} \perp \mathbf{B}$ zone.

In addition to the HARM and HAOM observations, high-altitude neutral Fe, Na, & K "layers" have been observed by lidar [5,6,7,8,11]. The hugely interesting Chu et al. [5] Fe-lidar results from McMurdo in Antarctica show apparently periodic descending Fe High-Altitude Metal Layers (HAMLs) that strongly resemble ionospheric descending intermediate layers such as those observed at Arecibo [6]. The suggested mechanism for these layers is electrodynamic pumping of Fe^+ from the ablative meteor zone followed by $Fe^+ \rightarrow Fe$ conversion via radiative recombination which implies a large ionosphere as this process is very inefficient. Results from Arecibo, shown

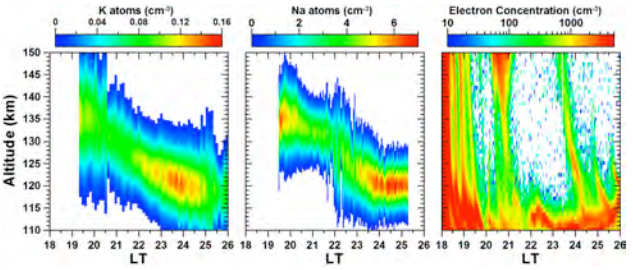

Figure 3. *UNIQUE* Arecibo *K*- & *Na*-lidar results compared with ISR electron concentration (N_e) results [6]. The left panels show the *K* and *Na* reconstructed thermospheric layers, respectively. The right panel displays the Tidal Ion Layers seen in the N_e data. Clearly, the ion and neutral layers are not coupled via ion-to-neutral conversion. We suggest that the neutral metal layers are "fossil" features of a bolide (large meteoroid) event.

in Fig. 3, show well-defined K- and Na-HAMLs that are not ionospheric in origin as demonstrated from the simultaneous incoherent scatter electron concentration results that show rapidly descending intermediate layers.

We suggest that the high altitude neutral metal layers are due to sputtering of fast meteoroids [2,3,4]. We next examine sputtering with particular attention to efficiency of O2/N2 and proton sputtering of Si, Fe, and Na.

3. Sputtering

In the meteoroid frame of reference, atmospheric molecules (N2/O2) of sufficient energy penetrate into the surface and collisionally dissipate kinetic energy while ejecting meteoroid atoms with production vs. incident collision efficiency [2] that is accessible to physics-based numerical experiments. In particular, plasma (and proton) sputtering is a highly-studied materials processing approach for which open-source simulation codes are readily available.

Figure 4 shows a Monte Carlo simulation of the linear collision cascade trajectories of 1000 individual 500 eV N2 molecules incident on solid sodium. A 300Å×300Å 2D cross section of this process is shown. At this energy level, equivalent to 77.65 km/sec, each incident N2 molecule yielded ~1 sputtered atom/ion. We assume an approximately equal sputtered atom vs. ion yield but this is an open issue. Sputtering yields for O2 and N2 are all ~0.3-0.5 at 40 km/sec, normal incidence impact speed onto Fe, Si, and Na and rise to ~1 at 60 km/sec.

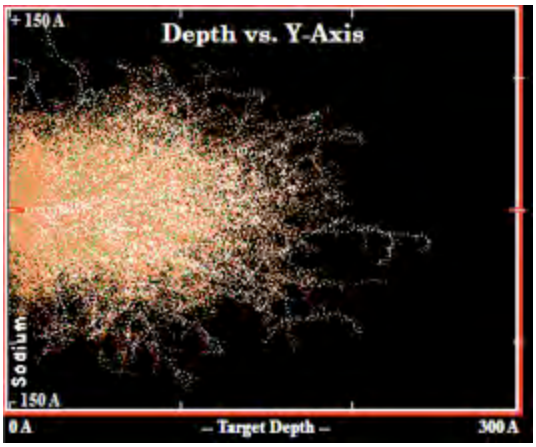

Figure 4. Monte Carlo simulation of energetic (500 eV=77.65 km/sec) N2 transport at normal incidence into solid sodium. Shown are the tracks of 1000 realizations of this process. At these energies the sputtering yield is ~1 sputtered atom/ion per incident N2. The SRIM (Stopping and Range of Ions in Matter) and the embedded TRIM (Transport of Ions in Matter) codes were used in these simulations. See: en.wikipedia.org/wiki/ Stopping_and_ Range_of_Ions_in_Matter

Relative to N2/O2 at the same 500 eV energy, protons readily penetrate into Fe, Si, and Na but the sputtering yield is very low (~0.02-0.12) due to the large mass ratio.

At lower energies proton sputtering is negligible, while at higher energies the sputtering yield increases some. Overall, for significant net proton sputtering a large proton flux and a large surface area of meteoroid material is required. We specifically address this issue below.

4. High-Altitude Radar Meteor Visibility

It is clear that both HAOMs and HARMs are being observed on a regular basis and that both are a product of sputtering of the faster (≥40 km/sec) meteoroids that occur as the apex of Earth's way rises at about midnight local time. Using the basic radar equation for point targets to estimate the sensitivity of the JRO 50 MHz radar [10], we determine that the minimum visible scattering cross-section for radar meteors for a given system temperature, etc. In this we employ the Radar backscattering Cross-Section (RCS) from N electrons, $\sigma_{BS} = 4\pi r_e^2 N^2$, which describes totally coherent scattering from N, equally illuminated and closely spaced ($\lesssim\lambda/4$ where $\lambda\simeq 6$ m for JRO), electrons where r_e is the classical electron radius. This calculation suggests that at least 10^{12} electrons are required for a radar meteor at ~150 km altitude. Figure 5 shows the cumulative number of atmospheric molecules

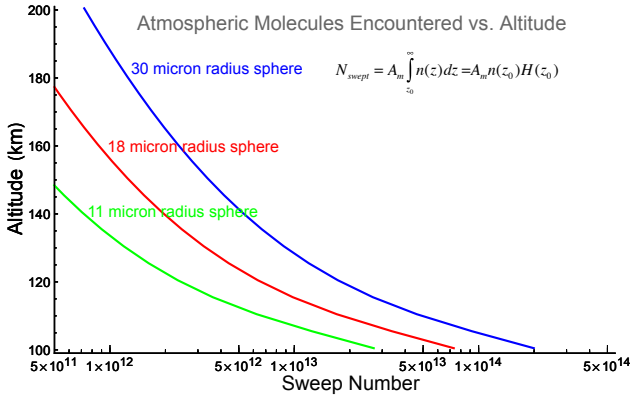

Figure 5. Number of atmospheric molecules encountered to altitude by a spherical particle of indicated radius. These are reasonable sizes for micrometeoroids. Note that ablation begins at ~110 km for the fastest micrometeoroids. For minimum radar meteor visibility [9,10] at least 10^{12} atmospheric molecules must be encountered assuming an ion sputtering yield of ~1 per collision for a fast meteoroid and that all sputtered ions (and electrons) remain in the vicinity of the meteoroid.

encountered to altitude from three *solid* spherical particles of indicated size. While these rough estimates are within the realm of possibility, it seems likely that the HARMs are visible as they are larger than 30 microns and/or they are icy or "dust ball" meteoroids that easily fragment thus presented a larger surface area to the atmosphere at high altitudes. The Figure 1 events suggests this possibility although that event was an optical bolide and thus (likely) noticeably larger than the sizes considered in Figure 5. Note that the atmospheric mean free path (MFP) ranges from ~10 cm at 100 km altitude to >100 m above 180 km and thus even cm-class meteoroids (bolides) are seen only via sputtering.

5. Lidar-Visible High Altitude Metals

Figure 6 shows a sodium-lidar High-Altitude Metal Layer (HAML) observed at the Andes Lidar Observatory (ALO), Cerro Pachón, Chile [8]. While the Na-HAML is of order 1-5 atoms/cc and is correspondingly difficult to detect, these results are compelling. In particular, we suggest that the onset of the HAML occurs at local midnight as the apex-of-Earth's way rises exposing the thermosphere is the fastest of the micrometeoroid flux and thus to sputtered sodium. The Figure 6 ALO results appear similar to those reported from the Gaomeigu Astronomical Observatory (GAO) in Lijiang (Yunnan), China [7]. The 4 nights of GAO observations are similar to Figure 6 especially when the time of solar midnight is noted.

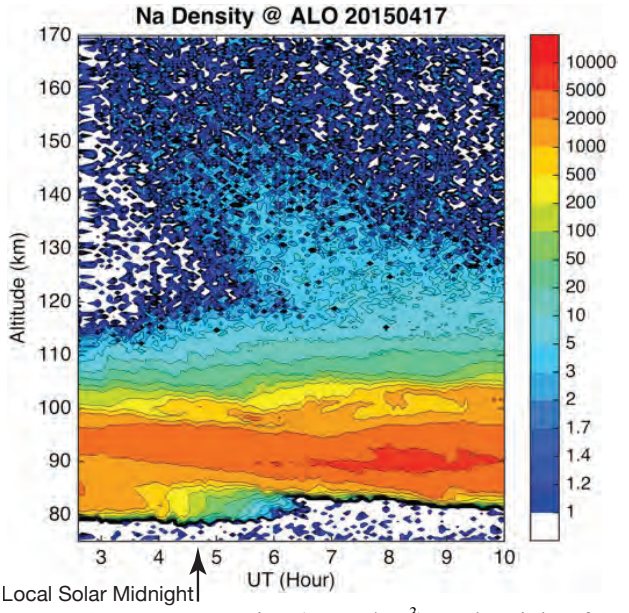

Figure 6. Na concentration (atoms/cm^3) on the night of 17 April 2015 measured by the Na lidar at the Andes Lidar Observatory in Cerro Pachón, Chile (UTC-4) [8, Figure 1]. This result is described as typical for those nights in which thermospheric Na was observed. Approximate local solar midnight (apex rise) is indicated. Note that a nonlinear color scale is used to highlight the low density in the thermosphere.

6. Discussion and Conclusions

That high-altitude optical and radar meteors are now observed is due to advances in instrumentation and signal processing along with observational paradigms that extend to ~200 km altitude. HAOM/HARMs must be due to sputtering of both optically-excited and ionized meteoroid atoms in, we assume for now, approximately equal proportions. Given the large MFP (>10 m) at these altitudes, secondary-collision optical excitation and ionization will be inefficient. In any case, the sputtering of fast meteoroids between apex rise (local solar midnight)

and dawn offers an explanation for Figure 6-like metals distributions in the 120-200 km thermosphere.

The Figure 3 Arecibo Observatory results show both Na- and K-HAMLs and, via simultaneous ISR electron concentration measurements, that the neutral metals are totally decoupled from the ionosphere. However, these AO HAMLs are well defined as layers over the whole observing period leading us to conclude that they are components of a "fossil" bolide trail. Other AO HAML observations more closely resemble Figure 6 [11]—ISR observations were not available in this case.

We contrast all of these results [6,7,8,11] with the Fe-HAMLs report at McMurdo [5] that do resemble the rapidly descending ionospheric intermediate layers shown in Figure 3. These Fe layers were attributed to electrodynamic pumping of Fe^+ from the ablative meteor zone followed by $Fe^+ \rightarrow Fe$ conversion via radiative recombination implying a large ionosphere as this process is very inefficient. In contrast, we hypothesize auroral (thus descending layer like appearance) proton sputtering of nanometer-sized meteoric dust derived from dusty/icy meteoroids and from the steady but invisible flux of small, slow interplanetary dust particles (IDPs) into the thermosphere. It seems certain that this hypothesized "reservoir" of meteoroid- and IDP-derived nanometer dust resides in the global thermosphere. The McMurdo Fe-HAML observations, along with satellite estimates of proton flux and energy spectrum offers a method of estimating the total sputtered surface area required to generate the observed Fe content.

Fast meteoroid sputtering of metals into the lower thermosphere and the suggested reservoir of nanometer-sized "dust" in the lower thermosphere likely form an important non-solar space weather feature along with the ablative meteor zone electrodynamic and chemical processes.

7. Acknowledgements

This work has been supported under NSF Grant AGS 12-41407 to Penn State and AO/SRI International. We thank PSU professor T.N. "Tom" Jackson for his insights into the sputtering process.

8. References

1. Spurný, P., H. Betlem, K. Jobse, P. Koten, and J. v. t. Leven (2000), New type of radiation of bright Leonid meteors above 130 km, *Meteor. Planet. Sci.*, *35*, 1109-1115, doi: 10.1111/j.1945-5100.2000.tb01497.x.

2. Popova, O. P., A. S. Strelkov, and S. N. Sidneva (2007), Sputtering of fast meteoroid's surface, *Adv. Space Res.*, *39*, 567-573, doi:10.1016/j.asr.2006.05.008.

3. Gao, B., and J. D. Mathews (2015), High-altitude meteors and meteoroid fragmentation observed at the Jicamarca Radio Observatory, *Mon. Not. R. Astron. Soc.*, *446*, 3404-3415, doi: 10.1093/mnras/stu2176.

4. Gao, B., and J. D. Mathews (2015), High-altitude radar meteors observed at Jicamarca Radio Observatory using a multi-baseline interferometric technique, *Mon. Not. R. Astron. Soc.*, *452*, 4252–4262, doi: 10.1093/mnras/stv1548.

5. Chu, X., Z. Yu, C. S. Gardner, C. Chen, and W. Fong (2011), Lidar observations of neutral Fe layers and fast gravity waves in the thermosphere (110–155 km) at McMurdo (77.8°S, 166.7°E), Antarctica, *Geophys. Res. Lett.*, *38*, L23807, doi: 10.1029/2011GL050016.

6. Raizada, S., C. M. Brum, C. A. Tepley, J. S. Friedman, J. D. Mathews, and F. T. Djuth (2015), First Simultaneous Measurements of Na and K Thermospheric Layers along with TILs from Arecibo, Geophys. Res. Lett., 42, doi: 10.1002/2015GL066714.

7. Gao, Q., X. Chu, X. Xue, X. Dou, T. Chen, and J. Chen (2015), Lidar observations of thermospheric Na layers up to 170 km with a descending tidal phase at Lijiang (26.7°N, 100.0°E), China, *J. Geophys. Res. Space Phys.*, *120*, 9213–9220, doi: 10.1002/2015JA021808.

8. Liu, A. Z., Y. Guo, F. Vargas, and G. R. Swenson (2016), First measurement of horizontal wind and temperature in the lower thermosphere (105–140 km) with a Na Lidar at Andes Lidar Observatory, *Geophys. Res. Lett.*, *43*, 2374–2380, doi: 10.1002/2016GL068461.

9. Mathews, J. D., D. D. Meisel, K. P. Hunter, V. S. Getman, and Q. Zhou (1997), Very high resolution studies of micrometeors using the Arecibo 430 MHz radar, *Icarus*, *126*, 157-169, DOI: 10.1006/icar.1996.5641.

10. Mathews, J. D. (2004), Radio science issues surrounding HF/VHF/UHF radar meteor studies, *J. Atmos. Solar-Terr. Phys.*, *66#3*, 285-299, doi:10.1016/j.jastp.2003.11.001.

11. Friedman, J. S., X. Chu, C. G. M. Brum, and X. Lu (2013), Observation of a thermospheric descending layer of neutral K over Arecibo, *J. Atmos. Solar-Terr. Phys.*, *104*, 253-259, doi: 10.1016/j.jastp.2013.03.002.